Measurement of thin liquid film thickness in pipes based on optical interferometry*

XUE Ting** **and WU Yan**
School of Electrical and Information Engineering, Tianjin University, Tianjin 300072, China

(Received 11 February 2022; Revised 7 April 2022)

Accurate measurement of the thin liquid film thickness in pipes is the foundation for studying the characteristics of the film. In this paper, an interferometry-based measurement of liquid film thickness in transparent pipes is developed, which can greatly improve the accuracy, extend the lower limit of measurement and provide a new technical approach for the calibration and traceability. The light intensity distribution is established based on the optical path analysis and a mathematical model. A new algorithm to solve the direction ambiguity is developed to reconstruct the phase distribution. Besides, the effect of the pipe wall is taken into account, which can be suppressed by image subtraction and enhancement technology. The proposed method is of high accuracy and robustness, whose reconstruction errors are 0.064% and 0.25% for the smooth and slight fluctuating liquid films, respectively.
Document code: A **Article ID:** 1673-1905(2022)08-0489-6
DOI https://doi.org/10.1007/s11801-022-2022-9

Gas-liquid two-phase flow is common in various industries, such as oil transportation, evaporators, condensers, and nuclear reactor cooling processes[1,2]. Accurate monitoring of liquid film characteristics is of great importance to ensure production safety and improve production efficiency. Liquid film characteristics include liquid film thickness, flow rate, and fluctuation characteristics, among which liquid film thickness is the basis for studying liquid film characteristics.

The existing liquid film thickness measurement methods mainly include ultrasonic methods, electrical methods, optical methods, and radiation methods[3]. Most ultrasonic methods use ultrasonic transducers, and are suitable for measuring thicker liquid film. For example, WADA et al[4] proposed an ultrasound technique to identify two-phase flow as well as measure the thickness and velocity of the annular flow liquid film. Electrical methods realize the measurement by the relationship between the current and the liquid film thickness. WOLF et al[5] set a conductivity probe to measure the liquid film thickness of the annular flow in a vertical upward pipe with an inner diameter of 31.8 mm. However, calibration is necessary to establish the relationship. Besides, the conductivity probe is invasive, and its spatial resolution and accuracy are limited[6]. In recent years, non-invasive methods, represented by optical methods[7-11], have developed rapidly, which can not only provide a new way for calibration, but also improve the spatial resolution and measurement accuracy. Interferometry is a major branch of the optical methods, which is widely utilized for thin film thickness measurement. SHANG et al[12] measured the thickness of a static ethanol film and an impinging sheet with partial coherent interferometry in a Mach-Zehnder interferometer. REN et al[13] obtained the thickness distribution of transparent glass film with multi-wavelength phase-shift extraction method in a large lateral shearing interferometer. CHEN et al[14] studied the microlayer structure of thin liquid film under boiling bubbles during nucleation boiling on the basis of laser interferometry. As a high-precision and high-sensitivity measurement method, interferometry provides a new approach for the calibration of thin liquid film thickness in pipes and simultaneously extends the lower measurement limit.

The purpose of this paper is to develop an interferometry-based measurement of liquid film thickness in gas-liquid two-phase flow, thereby improving the accuracy, extending the lower limit and providing a new calibration and traceability method. On the basis of optical path analysis, a mathematical model of light intensity distribution is established. A directional-ambiguity removal algorithm to reconstruct the phase is developed, which is of high accuracy and robustness. Moreover, the effect of the pipe wall is studied, which can be reduced through image subtraction and enhancement technology. Finally, different distributions of liquid film are considered and the reconstruction errors are evaluated.

The principle of interferometric measurement of liquid film thickness is shown in Fig.1. A laser beam illuminates the liquid film through the beam splitter and is

* This work has been supported by the National Natural Science Foundation of China (Nos.62071325 and 61828106).
** E-mail: xueting@tju.edu.cn

reflected on the two surfaces of the liquid film. Due to the optical path difference (*OPD*), the two beams of reflected light will interfere and be recorded by the high-speed camera through the beam splitter.

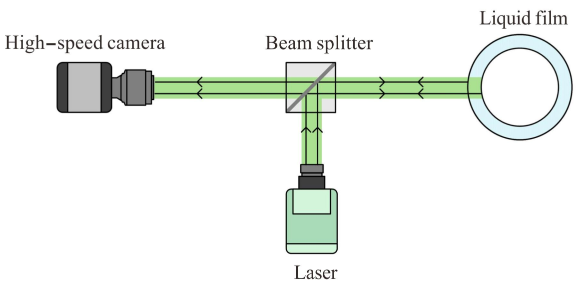

Fig.1 Schematic diagram of the interferometric method for measuring the liquid film thickness

The reflected light is analyzed by geometric optics, and the optical path diagram is shown in Fig.2. Assume that the inner radius of the pipe is R_1, the thickness of the film is R_1-R_2, the distance from the screen to the inner pipe wall is represented in the diagram as $OP=d$, the refractive index of air is n_1, and the refractive index of the liquid is n_2.

The reflection from the external surface is considered first. Assuming that the incident angle is i_0, the position of the reflected light on the screen can be expressed as

$$y_1 = OE' = R_1\sin i_0 + [d + (R_1 - R_1\cos i_0)]\tan 2i_0 \approx R_1 i_0 + 2d i_0 . \quad (1)$$

Since i_0 is very small, assume that $\sin i_0 = i_0$, $\tan 2i_0 = 2i_0$, and $\cos i_0 = 1$, and then the *OPD* can be denoted as

$$\varDelta_1 = n_1\left(d + \left(R_1 - R_1\cos i_0\right)\right)\left(1 + \frac{1}{\cos 2i_0}\right) + \frac{\lambda}{2} . \quad (2)$$

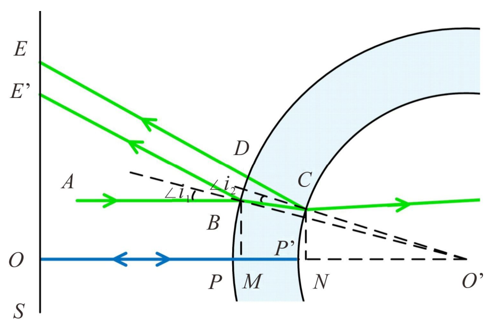

Fig.2 Optical path diagram of the light reflected from two surfaces of the liquid film

Due to the half-wave loss of the reflected light from the optically thin medium to the optically dense medium, $\lambda/2$ is added.

Considering the reflected light at the gas-liquid interface, the incident angles are assumed to be i_1 and i_2 on the external surface and the inner surface, respectively. The position of the reflected light on the screen is

$$y_2 = OE = R_1\sin i_1 + \left(d + \left(R_1 - R_2\cos i_2\right)\right)\tan 2i_2 \approx R_1 i_1 + \left(d + R_1 - R_2\right)\times 2i_2 . \quad (3)$$

As in the law of sines, we have $i_2 \approx (R_1/R_2)\, i_1$. Substitute this into Eq.(3), and we can get

$$y_2 = \frac{2R_1\left(d + R_1 - \frac{1}{2}R_2\right)}{R_2} i_1 . \quad (4)$$

The *OPD* can be written as

$$\varDelta_2 = n_1\left(d + R_1 - R_1\cos i_1\right) + 2n_2\left(R_1\cos i_1 - R_2\cos i_2\right) + n_1\left[\frac{d + R_1 - R_2\cos i_2}{\cos 2i_2} - \left(R_1\cos i_1 - R_2\cos i_2\right)\right] . \quad (5)$$

Assume that the two beams of reflected light meet on the screen, that is, $y_1=y_2$, so i_1 can be calculated from i_0 as

$$i_1 = \frac{(R_1 + 2d)R_2}{2R_1(d + R_1 - \frac{1}{2}R_2)} i_0 . \quad (6)$$

The phase difference between the two beams of light at the encounter point is obtained as

$$\Delta\varphi = \frac{2\pi}{\lambda}\left(\varDelta_2 - \varDelta_1\right) . \quad (7)$$

The amplitude of the incident light is assumed to be A_0. According to the definition of amplitude transmissivity and reflectivity, the amplitude of the reflected light can be calculated as

$$A_1 = \frac{n_2 - n_1}{n_2 + n_1} A_0 , \quad (8)$$

$$A_2 = \frac{4n_1 n_2 (n_1 - n_2)}{(n_2 + n_1)^3} A_0 . \quad (9)$$

Finally, the light intensity on the screen is confirmed to be

$$I = A_1^2 + A_2^2 + 2A_1 A_2 \cos\Delta\varphi . \quad (10)$$

As seen in the previous analysis, the phase difference $\Delta\varphi$ is the cosine function of the light intensity, and the light intensity is maximum when $\Delta\varphi = \pm 2k\pi$. Therefore, the phase difference between every two adjacent fringes in the interferogram is 2π, and the phase can be reconstructed according to the interferogram. However, the tendency of the phase across the fringe pattern is still unclear, leaving two possibilities (increasing or decreasing). There exists a problem of directional ambiguity.

A one-dimensional phase extraction algorithm is introduced in this paper, as only a one-dimensional distribution of the liquid film (along the pipe) is supposed to be obtained. The flow chart of phase distribution extraction is shown in Fig.3. Firstly, the image is converted to a grayscale image using the weight-average method. The middle column is extracted and filtered by a Gaussian filter in order to reduce the effect of the noise. Then, all the peaks of the light intensity are extracted. Since the light intensity distribution conforms to the cosine function, the majority of the peak values are almost equal.

However, as a result of the change in phase direction, a minority of the peak values are smaller than the rest, as shown in Fig.4.

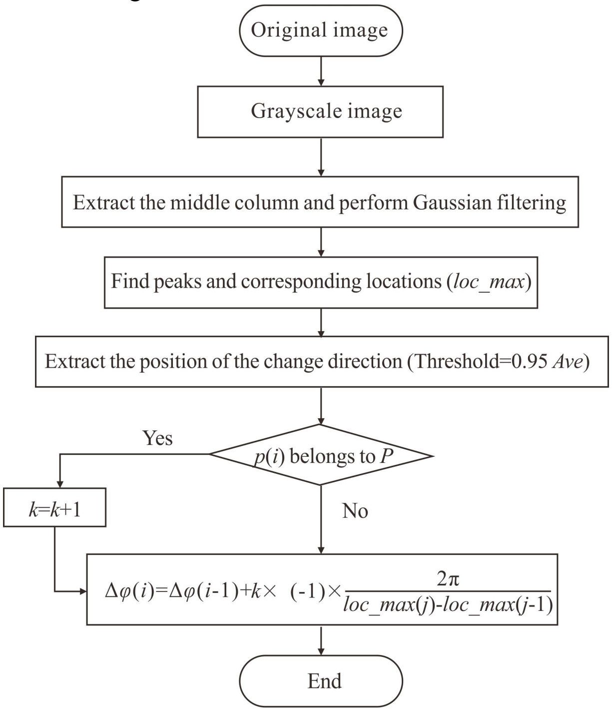

Fig.3 Flow chart of the directional-ambiguity removal phase distribution extraction algorithm

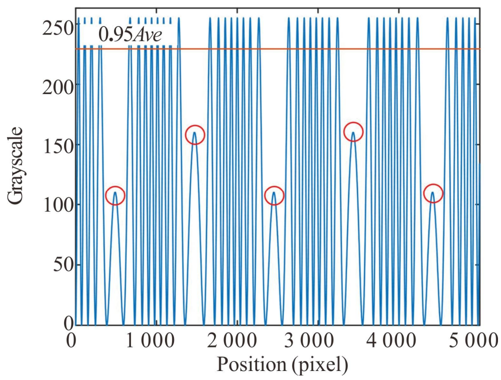

Fig.4 Light intensity distribution in the case of phase direction changing

To find the position where the direction changes, the threshold is set to 0.95 times of the average of all peak values (0.95*Ave*), and the peak values smaller than the threshold are all extracted, as are their positions. The positions are stored in a matrix ***P***, and for each position $p(i)$, whether $p(i)$ belongs to ***P*** is determined. The phase of each point can be calculated according to

$$\Delta\varphi(i)=\Delta\varphi(i-1)\pm\frac{2\pi}{loc\_max(j)-loc\_max(j-1)}, \quad (11)$$

where $\Delta\varphi(i)$ represents the phase difference between the two beams of light corresponding to the i-th pixel, and $loc\_max(j)$ represents the position of the j-th maximum.

According to the extracted phase, the *OPD* can be obtained, and then the liquid film thickness can be reconstructed. The relationship between *OPD* and phase difference $\Delta\varphi$ is as follows

$$\Delta\varphi=\frac{2\pi}{\lambda}OPD, \quad (12)$$

where λ is the wavelength of the laser. On the basis of Fermat's principle, the *OPD* is the product of the geometric path and the refractive index of the medium. Supposing that the refractive index of the liquid film is n, the formula for calculating the thickness of the liquid film can be written as

$$d=\frac{OPD}{2n}=\frac{\Delta\varphi\lambda}{4\pi n}. \quad (13)$$

Interferometric measurement converts tiny changes in thickness into more obvious changes in interference fringes so as to achieve higher sensitivity. For each level of interference fringe movement, the corresponding *OPD* changes by λ and the corresponding liquid film thickness changes by $\lambda/2n$. The sensitivity of the method can be defined as

$$S=\frac{4\pi n}{\lambda}. \quad (14)$$

When the laser wavelength is 532 nm and the refractive index of the liquid to be measured is 1.333, the sensitivity is 3.149×10^7 rad/m.

Such a high sensitivity leads to poor stability of the measurement system, and some small disturbances may affect the measurement results. Therefore, the entire experiment should be completed on a vibration isolation table. The room temperature should remain constant throughout the measurement, and there should be no airflow, ensuring the stability of the interferogram.

The flow is developed in a pipe, which is different from that on a glass plate or in a rectangular channel, where interference will not occur under normal incidence. The pipe wall, however, will affect the interferogram in the pipe flow due to its thickness and curvature. Multiple-beam interference is simulated to investigate the effects of the glass pipe wall on the interferogram. The stripes caused by the wall of the tube and the liquid film are perpendicular to each other and can therefore be distinguished very well. Negative effects of the tube wall on the interferogram are suppressed by image subtraction and contrast stretching as shown in Fig.5.

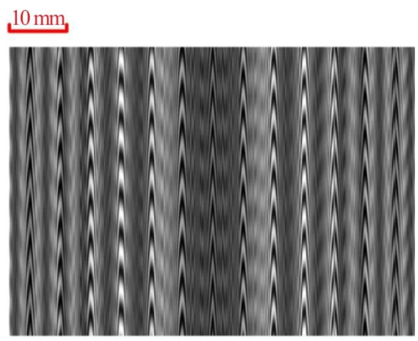

(a)

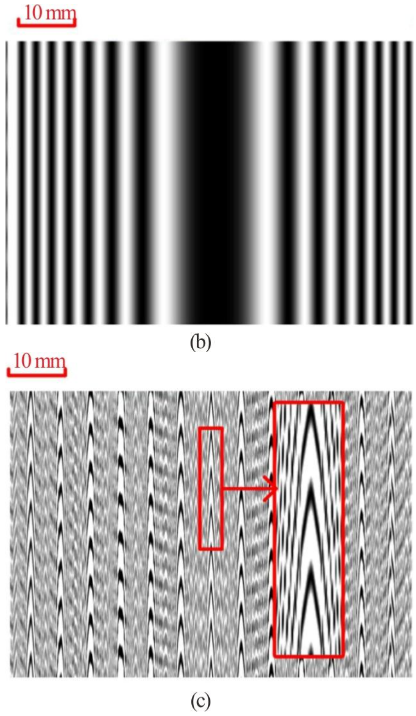

Fig.5 Multiple-beam interferograms: (a) Original interferogram; (b) Interferogram produced by the wall of the glass pipe; (c) Interferogram after processing

The effect of the pipe wall can also be eliminated through equipment such as the correction box. For example, WANG et al[15] used glycerol ($C_3H_8O_3$) to reduce the effect of light reflection on the surface of the glass pipe. It is reasonable to assume that the reflection from the outer wall of the pipe can be ignored, so the model can be simplified as a two-beam interference system.

In the two-beam interference system, an incidence beam is divided into two beams when it reaches the pipe. One is reflected on the inner pipe wall, while the other passes through the liquid film and is reflected at the gas-liquid interface. To verify the interferometric measurement of liquid film thickness and evaluate the performance of the phase extraction algorithm, liquid film with different thickness distributions is studied.

Suppose that the inner diameter of the glass pipe is 25 mm, the refractive index of the liquid is n_{liquid}=1.333, the laser wavelength is λ=532 nm, and the distance from the glass pipe to the camera is d=50 cm. According to Eq.(10), the light intensity received by the camera can be acquired. Then, the light intensity is converted to a digital signal to simulate the real conversion that occurs in the high-speed camera. The data format of the obtained images is 8-bit and the analogue light intensity is linearly mapped to the range from 0 to 255, with a rounding operation ensuring that the digital signal is an integer value.

When the thickness of the liquid film does not change, due to the curvature of the pipe, vertical interference fringes are generated along the radial direction of the pipe without fringes in the horizontal direction, as shown in Fig.6.

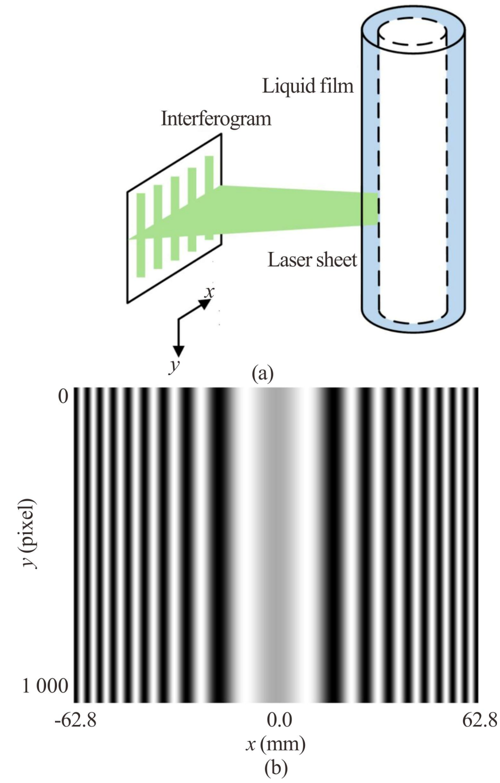

Fig.6 (a) Schematic diagram of interference generation; (b) Interferogram when the thickness of the liquid film is constant

Moreover, the smooth and slight fluctuating liquid films along the radial direction of the pipe are studied, and the interferograms are shown in Fig.7(a) and (b), respectively. In Fig.7(a), point A and point B are on the same interference fringe, so the phase differences at these two points are the same. The OPD and phase difference at point C are greater than those at point B. As a result, the phase difference at point C is greater than that at point A, which means the OPD at point C is greater than that at point A, and the liquid film at point C is thicker than that at point A. Along the positive direction of the y-axis, the film becomes thicker. In Fig.7(b), it can be analyzed that the liquid film at point C' is thicker than the liquid film at point A' in the same way. Along the positive direction of the y-axis, the thickness of the liquid film decreases and then increases.

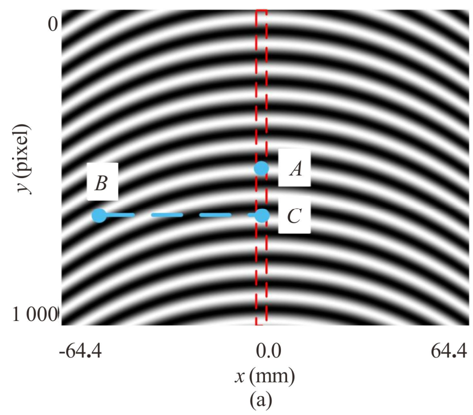

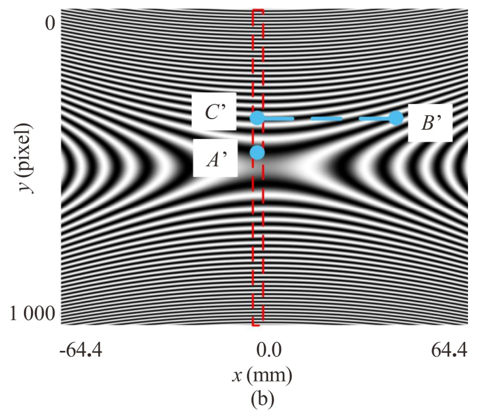

Fig.7 Two-beam interferograms: (a) Smooth liquid film; (b) Slight fluctuating liquid film

For the variation of the liquid film thickness along the axial direction of the pipe, only the middle column of the interferogram is taken (for example, the position marked with a red box in Fig.7). Utilizing the phase extraction algorithm proposed, the exact distribution of the liquid film thickness is obtained, as shown in Fig.8. The reconstruction error for the liquid film thickness is calculated as follows

$$E=\frac{\| d_{\mathrm{rec}}-d_{\mathrm{real}} \|_2}{\| d_{\mathrm{real}} \|_2}\times 100\%, \tag{15}$$

where $\|\cdot\|_2$ is the norm 2 operator, d_{rec} is the reconstructed liquid film thickness, and d_{real} is the actual liquid film thickness. The error for the smooth liquid film is 0.064%, and the error for the slight fluctuating liquid film is 0.25%.

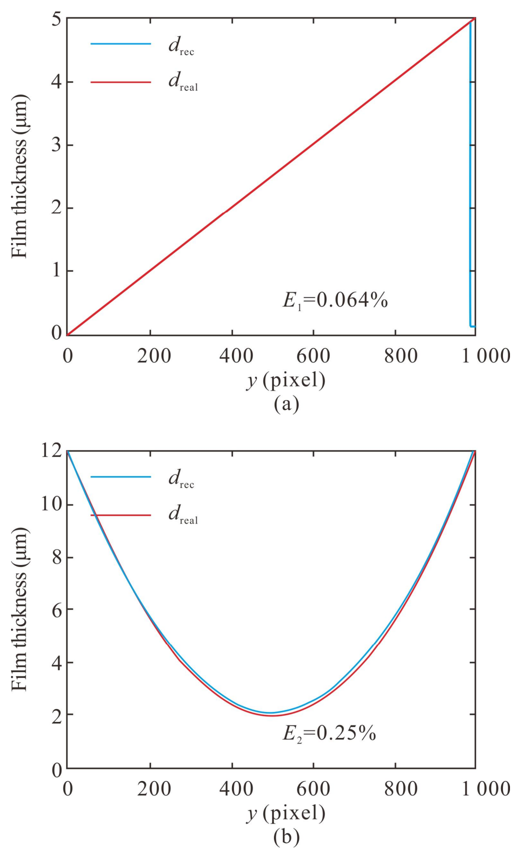

Fig.8 Distributions of liquid film thickness: (a) Smooth liquid film; (b) Slight fluctuating liquid film

In order to evaluate the immunity of the algorithm to noise, different levels of random noises are applied to the simulated light intensity signal. The standard deviation of noise is proportional to the light intensity, ranging from 0 to 30% with a step size of 5%. For each noise level, 10 sets of errors are obtained. The average values of the errors under all noise levels are shown in Fig.9.

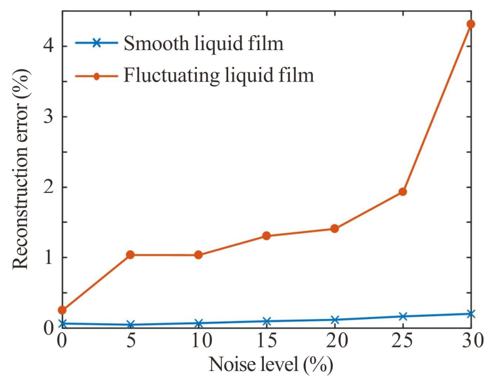

Fig.9 Variation of the mean values of the errors for 10 repetitions of the simulation, with noise levels varying from 0% to 30%

As the noise level increases, the measurement error of the liquid film thickness also increases. For the smooth liquid film, the measurement error of the liquid film thickness is less than 0.5%. When the thickness of the liquid film fluctuates, the error caused by noise increases. When the noise level is less than 25%, the error is less than 2%, but when the noise level is 30%, the error reaches 4.3%. The reason is that the phase involves a change in direction under the circumstances, which may cause an error. In general, the phase extraction algorithm applied in this paper is of high accuracy and robustness.

In conclusion, due to the high accuracy and low measurement limit, the interferometry-based measurement of liquid film thickness in gas-liquid two-phase flow is expected to become a competitive approach for the calibration and traceability of thin liquid film in pipes. The optical path is analyzed, and a mathematical model is established. A new reconstruction algorithm is proposed to eliminate the directional ambiguity in the reconstruction of the phase distribution. Multiple-beam interference is discussed to investigate the effect of the glass pipe wall on the interferogram, and pipe-induced fringes can be eliminated by image subtraction and enhancement technology. The reconstruction errors are 0.064% and 0.25% for the smooth and slight fluctuating liquid films, respectively. Furthermore, errors under different noise levels are analyzed to verify the robustness of the method.

Statements and Declarations

The authors declare that there are no conflicts of interest related to this article.

References

[1] XUE T, XU L S, ZHANG S Z. Bubble behavior characteristics based on virtual binocular stereo vision[J]. Optoelectronics letters, 2018, 14(1)：44-47.

[2] ZHOU X G, JIN N D, WANG Z Y, et al. Temporal and spatial evolution characteristics of gas-liquid two-phase flow pattern based on image texture spectrum descriptor[J]. Optoelectronics letters, 2009, 5(6)：445-449.

[3] XUE T, LI Z, LI C, et al. Measurement of thickness of annular liquid films based on distortion correction of laser-induced fluorescence imaging[J]. Review of scientific instruments, 2019, 90(3)：033103.

[4] WADA S, KIKURA H, ARITOMI M. Pattern recognition and signal processing of ultrasonic echo signal on two-phase flow[J]. Flow measurement and instrumentation, 2006, 17(4)：207-224.

[5] WOLF A, JAYANTI S, HEWITT G F. Flow development in vertical annular flow[J]. Chemical engineering science, 2001, 56(10)：3221-3235.

[6] CHERDANTSEV A V, MARKOVICH D M. Evolution of views on the wavy structure of a liquid film in annular dispersed gas-liquid flow[J]. Journal of applied mechanics and technical physics, 2020, 61(3)：331-342.

[7] WEI J, XU X, ZHANG J, et al. Measurement of liquid film coverage on vertical plates with hydrophilic and structured surface treatments[J]. Industrial & engineering chemistry research, 2021, 60(9)：3736-3744.

[8] SHEDD T A, NEWELL T A. Automated optical liquid film thickness measurement method[J]. Review of scientific instruments, 1998, 69(12)：4205-4213.

[9] SCHUBRING D, SHEDD T A, HURLBURT E T. Planar laser-induced fluorescence (PLIF) measurements of liquid film thickness in annular flow. Part II：analysis and comparison to models[J]. International journal of multiphase flow, 2010, 36(10)：825-835.

[10] CHAROGIANNIS A, AN J S, VOULGAROPOULOS V, et al. Structured planar laser-induced fluorescence (S-PLIF) for the accurate identification of interfaces in multiphase flows[J]. International journal of multiphase flow, 2019, 118：193-204.

[11] YOUN Y J, HAN Y, SHIKAZONO N. Liquid film thicknesses of oscillating slug flows in a capillary tube[J]. International journal of heat and mass transfer, 2018, 124：543-551.

[12] SHANG W, CHEN J. A partial coherent interferometry for measuring the thickness of a dynamic liquid sheet[J]. International journal of multiphase flow, 2019, 116：15-25.

[13] REN Y, CAO Z, TANG X, et al. μm-resolution thickness distribution measurement of transparent glass films by using a multi-wavelength phase-shift extraction method in the large lateral shearing interferometer[J]. Optics express, 2019, 27(3)：2899-2914.

[14] CHEN Z, HU X, HU K, et al. Measurement of the microlayer characteristics in the whole range of nucleate boiling for water by laser interferometry[J]. International journal of heat and mass transfer, 2020, 146：118856.

[15] WANG X, QIU H. Fringe probing of liquid film thickness of a plug bubble in a micropipe[J]. Measurement science and technology, 2005, 16(2)：59.